International Conference on Applied Energy 2021
Nov. 29 - Dec. 5, 2021, Thailand/Virtual
Paper ID: 927

Clamping-Force Control of a Sensor-less Electro-Mechanical Brake Actuator in New-Energy Vehicles

Z. Xu[1*], Chris Gerada [2]

1 University of Nottingham, China Campus (Corresponding Author)

2 University of Nottingham, UK

ABSTRACT

The explosive growth of New-Energy Vehicles (NEV) worldwide, combined with heated development in autonomous driving industries, has introduced a new demand for more controllable and reliable vehicle braking systems. Nowadays, the electro-mechanical brake (EMB) system is replacing the hydraulic or pneumatic ones, with lower mechanical complexity, high reliability, better individual wheel control and lower service and operating costs. This paper is focused on achieving accurate clamping force control of a force sensor-less electro-mechanical braking system, with the major technical objectives being: to analyze existing clamping force control methods for sensor-less EMB systems, to achieve clamping force estimation for sensor-less EMB systems, and to experimentally verify that the developed clamping force control strategy is accurate and well controlled.

Keywords: Force estimation, electromechanical brake, motor drives

1. INTRODUCTION

Almost all road-going vehicles are equipped with power-assisted braking systems [1-5] where the operator's pedal movement is amplified to generate a sufficient braking force. On ICE (Internal Combustion Engine) vehicles with hydraulic braking systems, this is achieved by means of a vacuum booster, that is powered either by the vacuum generated by the combustion engine's air intake, or by a vacuum pump connected to the engine's accessory pulley. Vehicles with air brake systems rely on an air compressor, either connected to the engine's accessory pulley or powered by the vehicle's low-voltage electrical system, to create the high air pressures needed to produce sufficient braking power.

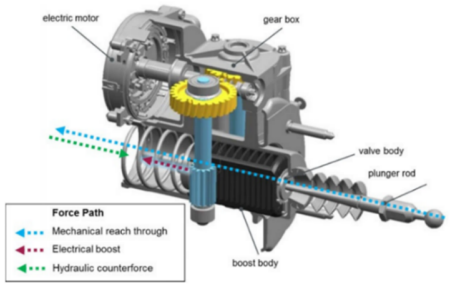

Fig. 1. An Electro-Mechanical Brake Booster

NEVs without ICE systems (Hydrogen Cell, Battery EV) do not have ICE air intakes, and thus cannot generate intake vacuum. Instead, high-voltage electro-mechanical brake boosters (Fig. 1) or vacuum pumps are used to complement existing hydraulic and air-based systems respectively. Thus, NEVs are still able to implement ABS [6] and TCS functions in a similar fashion to ICE vehicles.

This design is flawed, however, since the pumps may serve as a point of inefficiency and reduce the operational range of the vehicle by consuming energy originally reserved for traction use. They also present a challenge for autonomous driving development, as they introduce an additional point of failure into a vehicle's mechanical ecosystem and create actuation delays for emergency braking or traction control purposes.

1.1 Clamping Force Control, Sensored & Sensorless Systems

To realize accurate clamping force control, an EMB system may incorporate motor speed, motor current and brake pad pressure sensors as system parameter inputs. This is considered as a sensored system; the additional pressure sensors are not essential (but beneficial) for EMB operation. Sensored EMB systems are not suitable for practical use, however, as braking systems undergo harsh thermal and shock conditions. Brake pads on heavy

Selection and peer-review under responsibility of the scientific committee of the 13$_{th}$ Int. Conf. on Applied Energy (ICAE2021).

trucks and performance vehicles frequently reach 500 degrees Celsius during heavy braking [3], and heavy vehicles are often equipped with water cooling systems to rapidly reduce brake temperatures. Delicate electronics such as pressure sensors might not be able to operate under such high temperatures and dramatic thermal cycles, and their long-term reliability cannot be guaranteed. Brake calipers are part of the unsprung mass of a vehicle; in other words, brake calipers, usually located at the wheel hubs of a vehicle, do not benefit from the shock and vibration suppression effects of the vehicle's suspension system, and must endure mechanical stresses magnitudes greater than other sprung components. Thus, it can be said that a sensored EMB system allows for highly accurate clamping force control, albeit with lowered reliability and higher service costs.

For an EMB system [7-11] to be truly practical and commercially viable, it must be simplistic and reliable, yet functional and accurate. A sensor-less EMB system forgoes brake caliper pressure sensors and relies on motor current, position and speed readings for clamping force control, potentially achieving the same performance as a sensored EMB system with less components and lower cost. A sensor-less EMB system has the potential to usurp the long-established dominance of hydraulic and air-based braking systems, and usher in a new age of Electro-Mechanical braking.

2. EMB CONTROL WITH CLAMP-FORCE ESTIMATION

2.1 Torque - Balance Equation

To control clamping characteristics, EMB calipers can use a clamp force sensor for feedback. These sensors, however, must endure harsh environments (temperature, vibration, humidity), which reduces reliability while increasing costs for environmental hardening. Clamp force sensors can be substituted with a fusion of other on-board sensors, as proposed by Schwarz et al [5].

The first method utilizes the torque-balance equation, which assumes the clamping torque is equal to the sum of the actuator torque, the torque required to overcome the caliper's inertial effects and the torque required to overcome internal friction:

$$T_m = T_a + T_i + T_f \quad (1)$$

where T_m is the motor torque, T_a is the application torque, T_i is the torque that overcomes the inertial effects, and T_f the torque required to overcome internal friction. T_m, the motor torque, can be modeled as an ideal DC motor:

$$T_m = I_m \psi \quad (2)$$

where I_m is the motor current, and ψ is a constant representing the motor flux linkage. ψ can be modelled by varying the motor current I_m and measuring the resulting motor torque T_m, then graphing the results and obtaining the slope.

T_a , the application torque, can be derived as:

$$T_a = \gamma_{\text{tot}} F_{\text{cl}} \quad (3)$$

where γ_{tot} is the force amplificatory coefficient, and F_{cl} is the clamping force. T_i , the torque that overcomes the inertial effects, can be derived as:

$$T_i = J_{\text{tot}} d^2\theta_m/dt^2 \quad (4)$$

Where $d^2\theta_m/dt^2$ is the motor angular acceleration, and J_{tot} is the inertia. The motor angle θ_m is provided by a position sensor integrated in the motor. Thus, by combining (2)-(4), a relationship can be determined between motor current, clamping force, motor inertia and motor angle, as shown below:

$$T_m = \gamma_{\text{tot}} F_{\text{cl}} + J_{\text{tot}} d^2\theta_m/dt^2 + T_f \quad (5)$$

Equation (5) provides a highly accurate model for controlling an ideal EMB actuator. A practical actuator, however, is complicated both in its construction and in its operating environments, and an all-encompassing control model capable of taking in every possible variable will be impractical to develop.

2.2 Motor Angle Sensing

The second estimation method only requires one attribute: the motor's angle. A caliper characteristic curve is used to estimate the corresponding clamping force based on a specific motor angle. [5] This can be done with an encoder in the case of a brushed motor, or the phase wires of a BLDC motor, both methods widely adopted in the robotics and vehicular fields. The contact point, or "bite point" of the brake pad and rotor, however, must be defined beforehand, so as to define the motor angle at which clamping, thus braking, begins to occur. This point changes gradually as pad and rotor wear occurs, and is susceptible to user manipulation, such as when the user switches out the stock pads and rotors for aftermarket variants, thus altering the bite point of the braking hardware.

One solution to this issue is to "delay" the bite point motor angle as the brake pad wears [5], as shown in Fig. *2*. Other than the intercept with the horizontal axis, the characteristic curve remains unchanged. A possible method to finding the intercept, or the bite point, is to actuate the caliper either manually by user intervention or autonomously during vehicle shutdown and carry out automated diagnostics to determine the new bite point.

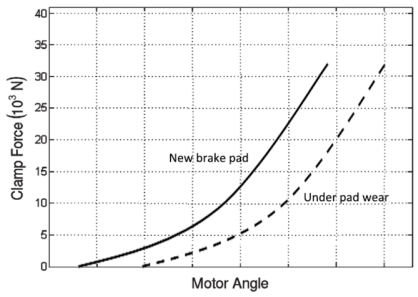

Fig. 2. Characteristic curves of a proposed EMB caliper [5]

The implementation of these methods, however, beyond the scope of this paper.

3. BRAKE CALIPER CLAMPING CHARACTERISTICS

To determine the characteristic curve of the brake caliper, the EMB module was connected to a computer-controlled bench power supply, where a current-control method was investigated and tested, with the initial assumption that the latter would be more suitable for this project.

3.1 Current Control of Clamping Force

The ability to control clamping force via current control was investigated. The input current was gradually ramped up from 1A to 15A with intervals of 1A. The input voltage was set to 12V at the power supply. To eliminate any residual clamping force and ensure that the clamping action at each current step was not assisted by the previous actuation, the EMB piston was retracted completely before testing at a new current step. It is assumed that at 0A, the EPB will not operate, and there will be no clamping force.

As shown in Fig. *3*, the EMB clamping force saw a relatively linear increase from 0A to 5A, plateauing at 10A and showed no increase from 10A to 15A. Thus, it can be said that the caliper's clamping force limit is at 10A, where it generates 11444N. Curve fitting was carried out to model this relationship, and the results are shown below:

$$F(a) = 0.049103a^4 - 3.311a^3 - 65.654a^2 + 2099.375a - 152.479 \quad (6)$$

Where $F(a)$ represents the Clamping Force, and a represents the Input Current from 0A to 10A. When $a \geq 10$, $F(a) = 11444N$.

Based on the relationship between motor input current and motor output clamping force, several adjustments were applied to achieve more steady and accurate force control. Firstly, because the input current sent from the motor shield to motor was modulated by PWM, the weight of the exponential filter was narrowed

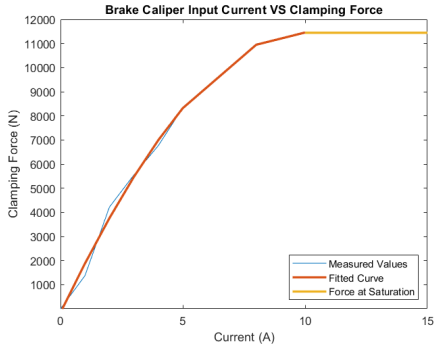

Fig. 3. Brake Caliper Input Current VS Clamping Force

to 9% for removing the spikes and pulses of the current to stabilize and smooth the PID control loop (Fig. *4*) as well as the force output [11]. Secondly, the output of the PID control loop was adjusted which was the main issue causing the incompletely releasing of motor clamping force.

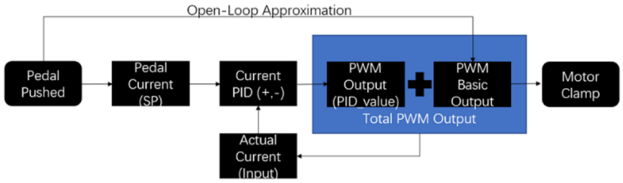

Fig. 4. The Algorithm of Closed-loop Current Control

3.2 Force Estimation

Practically, the viscous friction is smaller than Coulomb friction term, equation (5) can be re-written as:

$$T_m \approx \gamma_{tot} F_{cl} + J_{tot} d^2\theta_m / dt^2 + (\mu F_{cl} + A)\mathrm{sgn}(d\theta_m / dt) \quad (7)$$

where the Coulomb friction coefficient is defined as μ and the kinetic offset as A. A mathematical model for the mechanical dynamics is derived. $d\omega_m/dt$ is given from (7).

$$\frac{d\omega_m}{dt} = \frac{1}{J_{tot}}[T_m - (\mu F_{cl} + A)sgn(\omega_m) - \gamma_{tot} F_{cl}] \quad (8)$$

During clamping, $sgn(\omega_m) = 1$. (8) becomes:

$$\frac{d\omega_m}{dt} = \frac{1}{J_{tot}}(T_m - A) - \frac{\gamma_{tot}+\mu}{J_{tot}} F_{cl} \quad (9)$$

Let $g = -\frac{\gamma_{tot}+\mu}{J_{tot}} F_{cl}$. g represents the scaled aggregate of the clamping and frictional torque. Also, in the clamping and release actions, the associated uncertainties and perturbations are congregated in g. μ, γ_{tot}, J_{tot}, F_{cl} and unmatched parameters are confined by the EMB specifications and operating conditions. The magnitude of g will increase once the unidentified disturbance varies rapidly. For this purpose, the derivative of g is defined as $\dot{g} = w(t)$. $w(t)$ is

assumed to be bounded uncertainty. The mechanical dynamics of the motor is expressed as:

$$\begin{cases} \dot{\theta}_m = \omega_m \\ \dot{\omega}_m = \frac{1}{J_{tot}}(T_m - A) + g \\ \dot{g} = w(t) \end{cases} \quad (10)$$

An Extended Luenberger Observer (ELO) is built around (10). By utilizing the speed and torque equation, a 3rd order ELO can be constructed as follows.

$$\begin{cases} \dot{\hat{\theta}}_m = \hat{\omega}_m + l_1 e_\theta \\ \dot{\hat{\omega}}_m = \frac{1}{J_{tot}}(T_m - A) + l_2 e_\theta + \hat{z}_l \\ \dot{\hat{z}}_l = l_3 e_\theta \end{cases} \quad (11)$$

where $\hat{\theta}_m$ denotes the estimate of θ_m, and $e_\theta = \theta_m - \hat{\theta}_m$ is the difference between the measured and estimated rotor positions. $\hat{\omega}_m$ is the estimate of ω_m, and sgn(·) denotes the signum function. $\hat{z}_l$ is an extended state defined to estimate the clamp force term g in the system modelling (10). l_1, l_2 and l_3 are the observer gains that can be obtained by using the pole placement method. In frequency domain, the transfer function $G_{z-g}(s)$ between the extended state $\hat{z}_l$ and g can be deduced. A certain bandwidth ω_0 can be set to eliminate high frequency noises based on [12]. Since l_1, l_2 and l_3 are proportional to the distance from the poles of the plant to those of the observer, all the three poles of $G_{z-g}(s)$'s characteristic polynomial can be placed at ω_0.

$$s^3 + l_1 s^2 + l_2 s + l_3 = (s + \omega_0)^3 \quad (12)$$

where $l_1 = 3\omega_o;\ l_2 = 3{\omega_o}^2;\ l_3 = {\omega_o}^3$.

4. EXPERIMENTAL RESULTS

The Caliper test rig shown in Fig. *5* includes the control hardware and the EMB. 12VDC power is supplied by three 18650 Lithium-Ion cells in series. The L298N Motor Driver, insufficient in providing the full current demand of 10A, is replaced with a Custom Motor Driver capable of an output current of 14A. The Load Cell is placed on a custom-machined aluminum frame, which itself is attached to the caliper's left brake pad support. The left brake pad is removed while the right brake pad is flipped, allowing its metal backside to act as a load spreader for the load cell. The purpose of installing the load cell is just to provide a comparison between the estimated force and measured one and not used for the sake of force control.

The regular braking tests have been conducted with amplified current noises to verify the performance of the ELO. The measured and estimated forces produced by the observer are presented separately in Fig. *6*. By

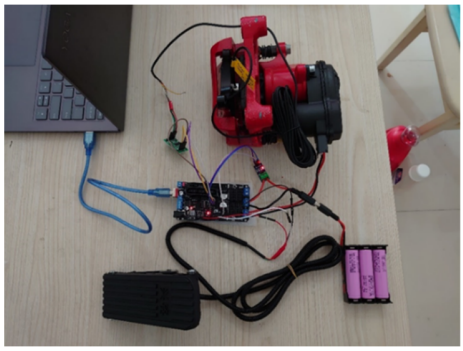

Fig. 5 Test Rig Layout

applying the fast Fourier transform, the frequency spectrums were obtained in Fig. *7*. The ELO can track the force variation frequency to around 90 Hz though some decay on the amplitude exists. It is obvious that the clamp force estimated by ELO match with the measured ones closely, which proves that the ELO has the significant advantage on the force estimation during both the steady-state and transients.

In Fig. *8*, the first pulse represents the clamping action, while the second pulse represents the retraction action. The measured current (Red) follows the current demand (Cyan) relatively closely, and the PD output (Pink) is actively compensating for any differences.

It is demonstrated in Fig. *9* that the closed-Loop control of current as well as its corresponding force was successfully matched the demand current and force. The Closed-Loop Current Control achieved the stable control with error less than 3% compared to the demand force and the response of motor was around 70ms. This result demonstrated the feasibility and practicability of the actuator force control strategy with current closed loop.

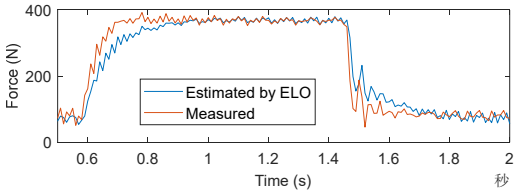

Fig. 6 The clamping force estimation in the regular braking mode: the measured force versus the estimated force by the ELO.

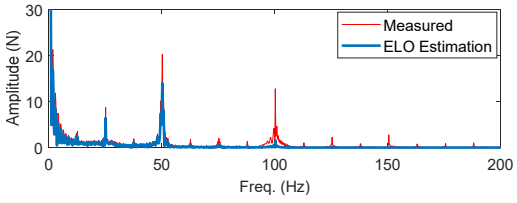

Fig. 7 The Frequency spectrum of the measure force and estimated one by the ELO.

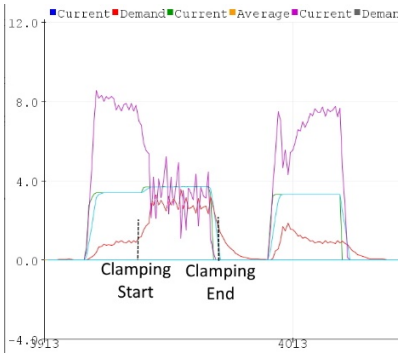

Fig. 8 One Actuation-Retraction Cycle, With Pedal, Current and Motor Speed Values

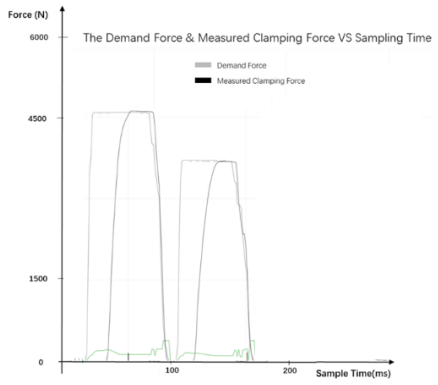

Fig. 9 Clamp-force control without force sensor

CONCLUSIONS

In this paper, the two main technical objectives, and their broken down tasks, of this project were accomplished as below:

1. Clamping force estimation for sensor-less EMB systems has been achieved, and the differencebetween the estimated and actual clamping force has been evaluated.
2. The developed clamping force control strategy has been verified to be accurate and well controlled by Implementing PID control of actuator current and estimating the clamping force under the closed-loop conditions without any force sensor.

ACKNOWLEDGEMENT

Supported by Zhejiang Provincial Natural Science Foundation of China under Grant No. LGG19E070009 and Ningbo Science and Technology Bureau under the project No. 202003N4182.

REFERENCE

[1] D. Frank, “Architecture for an electromechanical braking system” US Patent 8602505, Dec. 10, 2013.

[2] Bayer B. et al, “Electro-Mechanical Brake Systems” in Handbook of Driver Assistance Systems. Springer, Cham.

[3] Z. Dalimus, “Braking System Modeling and Brake Temperature Response to Repeated Cycle. Mechatronics, Electrical Power, and Vehicular Technology. 5. 10.14203/j.mev.2014.v5.123-128.”, 2014.

[4] W. Xiang. et al, “Automobile Brake-by-Wire Control System Design and Analysis”, *IEEE Transactions On Vehicular Technology*, vol. 57, no. 1, Jan. 2008

[5] Z. Wei. Et al, “Clamping Force Control of Sensor-less Electro-Mechanical Brake Actuator” in Proceedings of 2017 IEEE International Conference on Mechatronics and Automation, August 6 – 9, 2017, Takamatsu, Japan

[6] A. O. Moaaz Et al, “Investigation of Anti-Lock Braking System Performance Using Different Control Systems”, *International Journal Of Control And Automation*, vol. 13, no. 1s, 2020.

[7] V.A. Katić. Et al, “ELECTRIFICATION OF THE VEHICLE PROPULSION SYSTEM – AN OVERVIEW” University of Novi Sad, Faculty of Technical Sciences, Novi Sad, Serbia, Jun. 2, 2014.

[8] F. Un-Noor. Et al, “A Comprehensive Study of Key Electric Vehicle (EV) Components, Technologies, Challenges, Impacts, and Future Direction of Development”, *Energies*, 10(8), 1217, Aug. 17, 2017.

[9] S. Lambert, N. Kareta, "AUTOMOTIVE BUSINESS Corona Crisis: These automotive players are broke” mes-insights.com.

[10] *Electric Park Brake (EPB and EPBi)*, Conekt ZF TRW Technical Centre, Solihull, United Kingdom, 2015

[11] E. Ostertagová, Oskar Ostertag, “THE SIMPLE EXPONENTIAL SMOOTHING MODEL”, presented at the Modelling of Mechanical and Mechatronic Systems 2011 - The 4th International Conference, Herľany, Slovak Republic, Sep. 20 – 22, 2011.

[12] D. Yoo, S. S. T. Yau, and Z. Gao, "Optimal fast tracking observer bandwidth of the linear extended state observer," International Journal of Control, vol. 80, pp. 102-111, 2007.